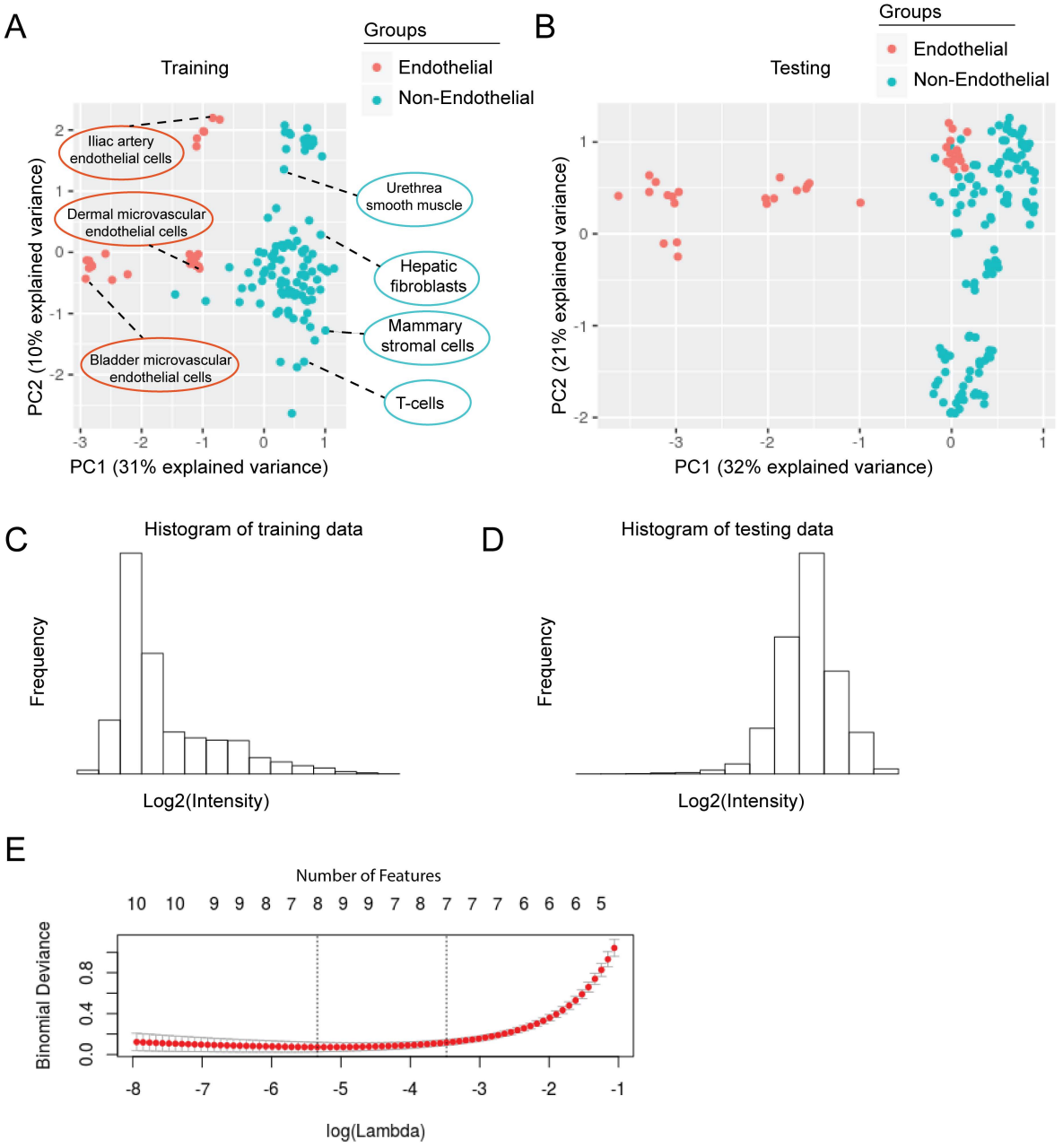


Supplemental Figure 1

**Supplemental Figure 1. Generating an endothelial cell classifier.** (**A-B**) Principle Component Analyses of the training (n=131) (**A**) and testing (n=139) (**B**) human microarray datasets. Endothelial cells dissected from various sources were classified as 'endothelial' (E), and non-endothelial cell populations representing other components of the tumor microenvironment were labeled 'non-endothelial' (N). Several representative microarray samples within the training set are labeled (**A**). Analysis of the testing set shows clear separation of the 'E' and 'N' classes by the first two components of the classifier, indicating that the results are not impacted by batch effects from the various sources of microarray samples. (**C-D**) Histograms of the training (**C**) and testing (**D**) microarray datasets approximate a normal distribution, indicating that separation of the 2 classes is not due to data handling. (**E**) K-fold cross validation was used to identify the optimal value for the penalty term 'lambda' in the ElasticNet model, which corresponded to a 7-gene endothelial classifier.

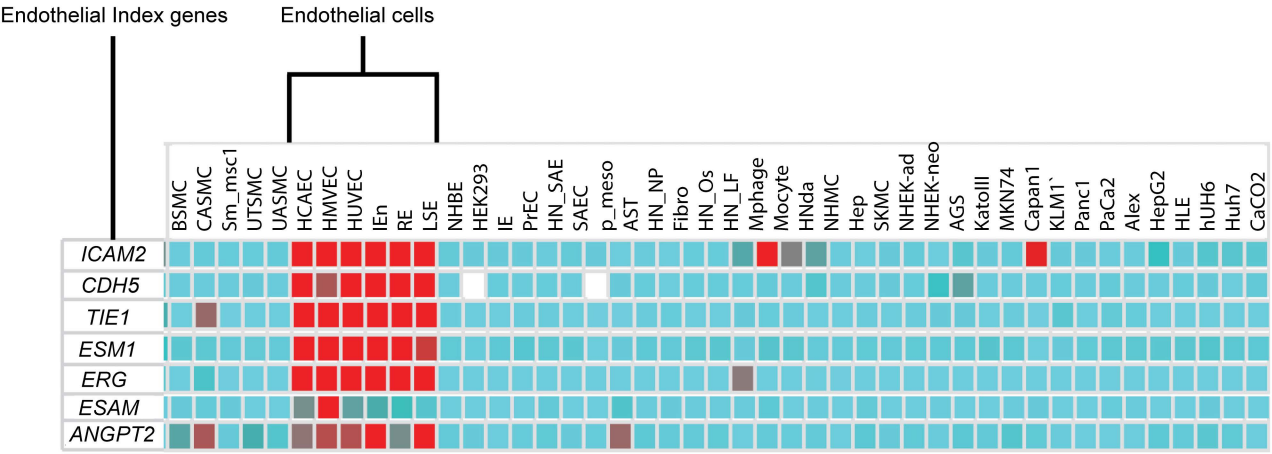


Endothelial cell types:

HCAEC: Human coronary artery endothelial cells
HMVEC:Human microvascular endothelial cells
HUVEC: Human umbilical vein endothelial cells
IEn: Intestinal endothelial cells
RE: Retinal endothelial cells
LSE: Liver sinusoidal endothelial cells

Supplemental Figure 2

**Supplemental Figure 2. Further tests of specificity for the endothelial index genes.**

Expression values of the endothelial index genes (*ICAM2, CDH5, TIE1, ESM1, ERG, ESAM* and *ANGPT2*) in the REFEXA database of human tissues (http://sbmdb.genome.rcast.u-tokyo.ac.jp/refexa/main_search.jsp). Gene expression is shown on a relative scale (0-200, red high, blue low).

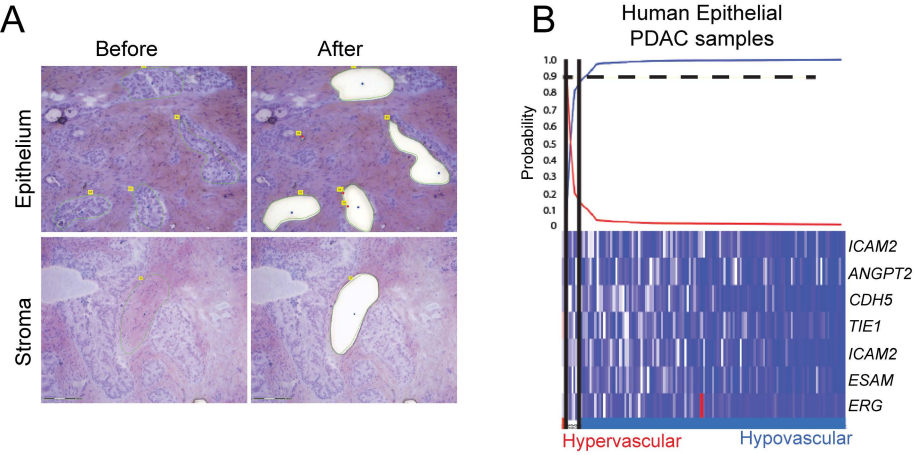


Supplemental Figure 3

**Supplemental Figure 3. Validation of the EI in micro-dissected PDAC tumor samples.** (**A**) Representative images showing the technical quality of tissue microdissection, before and after laser capture. Stroma and epithelium were isolated separately from 124 pancreatic adenocarcinomas (PDACs), generating a stromal sample and an epithelial sample for each tumor. RNA-sequencing was independently performed on these stromal and epithelial PDAC samples. (**B**) EI scores were calculated from the epithelial samples as a negative control (compare with Fig. 1d). Almost all samples were predicted to be hypo-vascular, consistent with the avascular nature of tumor epithelium. A single sample predicted to be hyper-vascular represented a biological outlier in the dataset (see Methods and ref (11)).

Representative staining
from multiple regions of the tumor

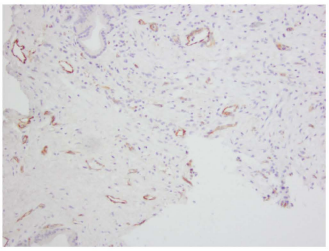

*CD31*
Hematoxylin

Split color channels

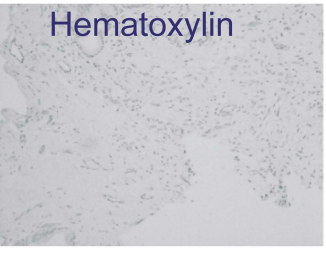


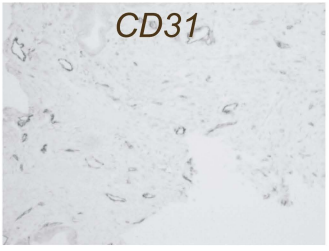


Quantify % area staining

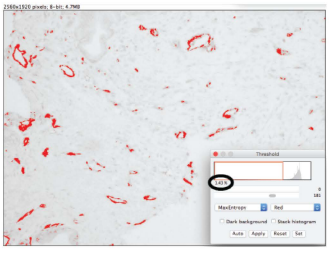

Supplemental Figure 4

**Supplemental Figure 4. Quantification of tumor microvessel density (MVD).** Formalin-fixed paraffin-embedded human PDAC samples were sectioned and stained for *CD31* with hematoxylin counterstain. To quantify MVD, the brown and purple color fields were separated using ImageJ, and the percent area of CD31 staining was calculated (N=44 tumors, 2 sections/tumor, 5 fields/section for each tumor).

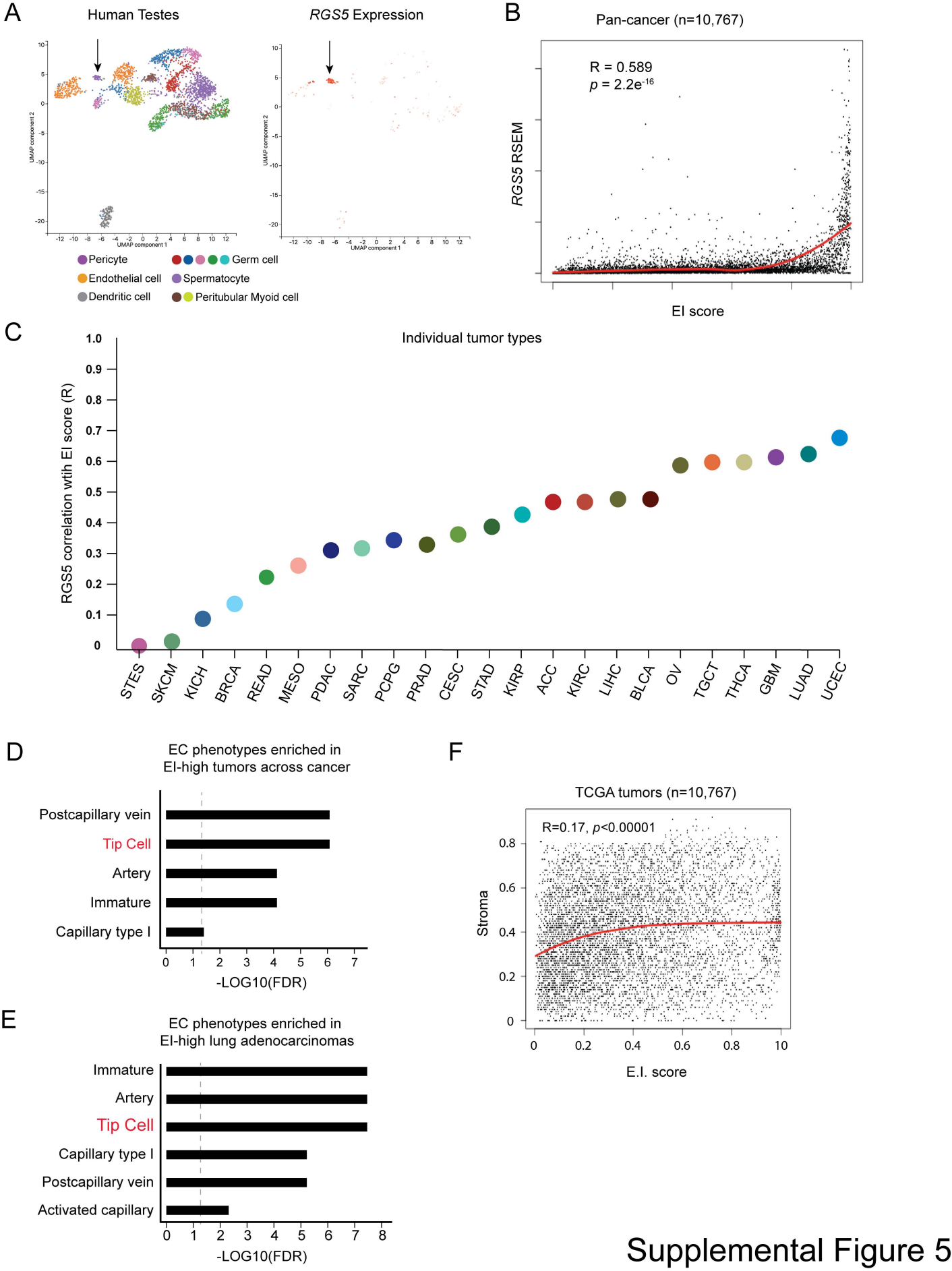


Supplemental Figure 5

**Supplemental Figure 5. EI score associates with expression of pericyte marker *RGS5* and with various endothelial subsets across cancer**

(**A**) UMAP plot showing scRNA-seq data of human testes. *RGS5* expression colocalizes specifically with the pericyte population (arrow). (**B-C)** Correlation coefficient (R) and corresponding 2-tailed probability values were calculated to test the relationship between EI score and *RGS5* expression in all tumors (**B**) and in individual tumor types (**C)**. Correlation between gene signatures for specific EC (endothelial cell) phenotypes and those for all solid tumors with high EI scores (**D**) and lung adenocarcinomas with high EI scores (**E**) were calculated using Fisher's exact test (dashed line signifies cutoff for statistical significance, *FDR*=0.05). (**F**) Scatterplot and smoothed Loess regression curve demonstrate the correlation between stromal content, estimated using the ESTIMATE algorithm and EI score in 10,767 solid tumors.

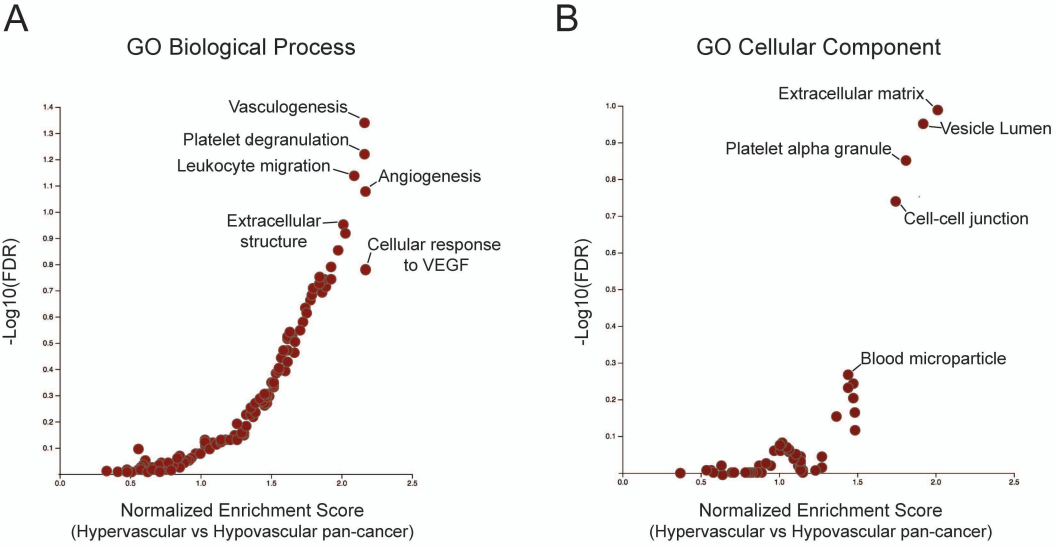


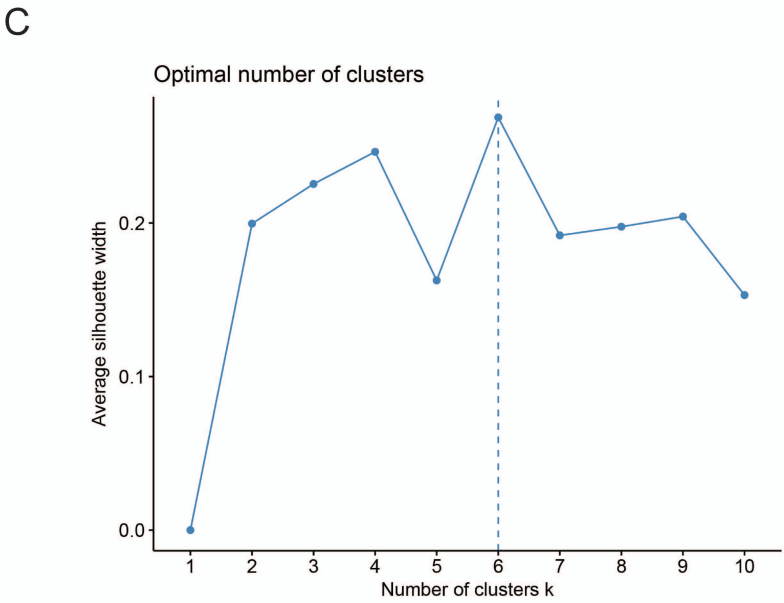


Supplemental Figure 6

**Supplemental Figure 6. A network of vascular hub genes allows stratification of tumors into six vascular-associated subtypes. (A-B)** Gene Set Enrichment Analysis (GSEA) of Biological Process (**A**) and Cellular Component (**B**) signatures up-regulated in tumors estimated to be highly vascular ($90^{th}$ percentile EI) across all cancer types. (**B**) The average silhouette method was used to determine the optimal number of clusters to group 10,767 solid tumors by their expression of 24 vascular 'hub' genes. A detailed explanation for the generation of 6 vascular subtypes is included in the Methods section.

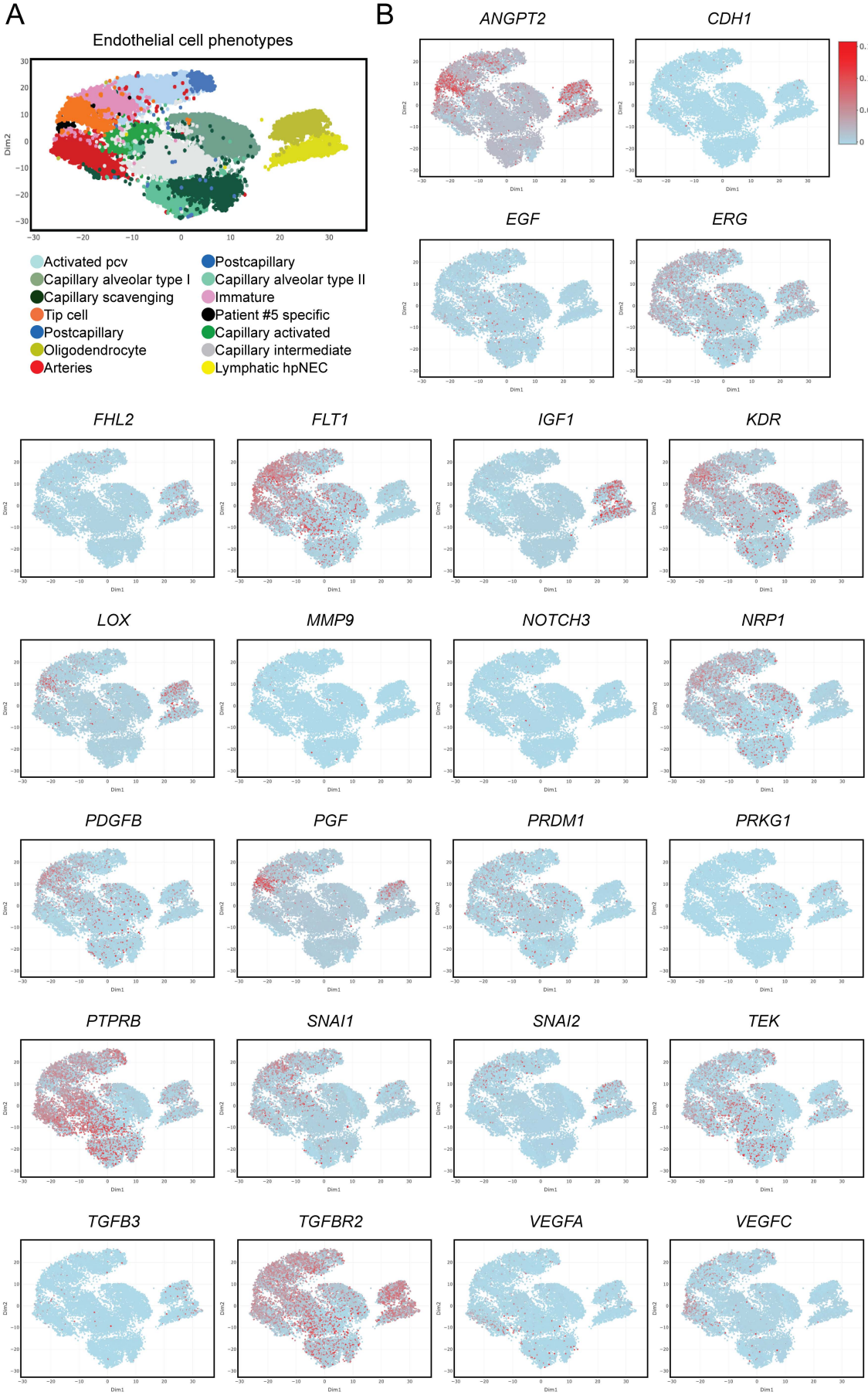


Supplemental Figure 7

**Supplemental Figure 7. Vascular hub genes exhibit varying levels of expression in endothelial cells**

**(A-B)** Individual malignant and normal lung endothelial cells are marked by their phenotypes as defined by Goveia et al. 2020 (**A**) or the expression of the 24 vascular signaling hub genes (**B**). Normalized expression levels are plotted on a relative scale from low (blue) to high (red).

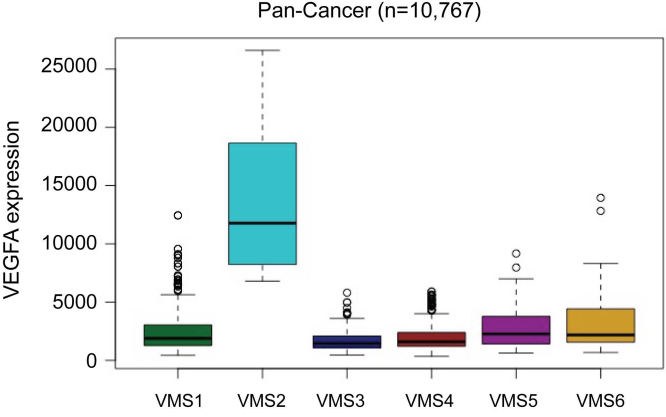


| | | | | | | |
|---|---|---|---|---|---|---|
| VMS2 | <2e-16 | — | — | — | — | — |
| VMS3 | 4.3e-15 | <2e-16 | — | — | — | — |
| VMS4 | 5e-9 | <2e-16 | 0.00038 | — | — | — |
| VMS5 | 0.0073 | <2e-16 | <2e-16 | 2e-14 | — | — |
| VMS6 | 1.4e-8 | <2e-16 | <2e-16 | <2e-16 | 0.0326 | — |

FDR pairwise comparisons (Kruskal-Wallis rank-sum test)

Supplemental Figure 8

**Supplemental Figure 8. *VEGFA* expression varies by VMS.**

Boxplots showing *VEGFA* expression of all solid tumors (TCGA) grouped by VMS (center line marks the median, box limits span the inter-quartile range, whiskers extend 1.5 times the inter-quartile range and black circles indicate outliers). *VEGFA* expression levels were compared across all 6 VMS subgroups. Significance of the difference in *VEGFA* expression between specific subgroups was tested by Kruskal-Wallis rank sum pairwise test and corrected for multiple comparisons with Benjamin-Hochberg (BH) adjusted post-hoc and presented as false discovery rates (FDR) in a table.

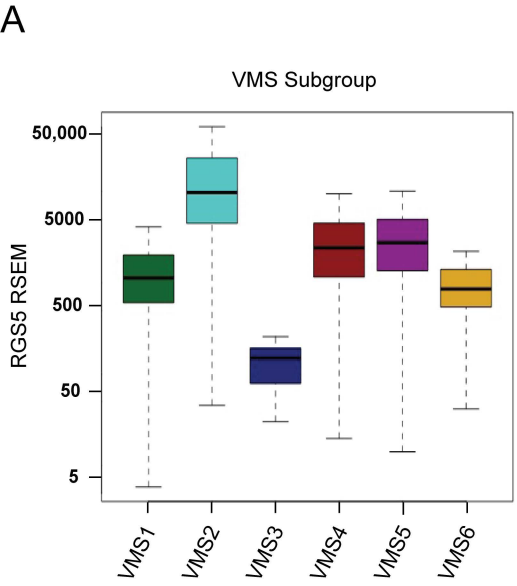


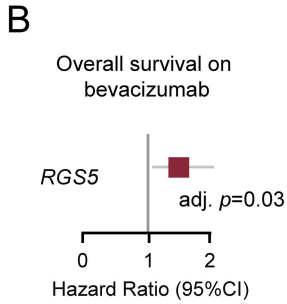


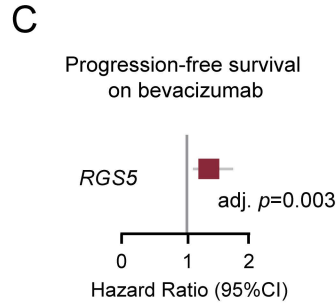


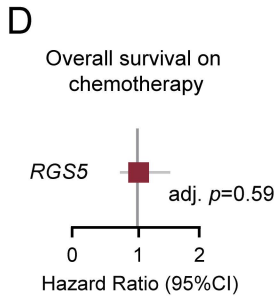


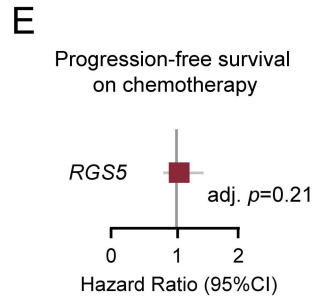


Supplemental Figure 9

**Supplemental Figure 9. Pericyte coverage, approximated by *RGS5* expression, varies by vascular subtype and associates with poor response to bevacizumab**

(**A**) Boxplots showing *RGS5* expression across the six vascular-microenvironment signatures. Boxplots: center line marks the median, box limits span the inter-quartile range, whiskers extend 1.5 times the inter-quartile range and black points indicate outliers. Forest plots showing the association of *RGS5* expression with overall (**B, D**) and progression-free (**C, E**) survival in ovarian cancer patients treated with bevacizumab or chemotherapy alone, respectively. A multivariate Cox model was used to calculate the hazard associated with *RGS5* in each scenario, with patient age and tumor stage as covariates. Hazard ratios are plotted on a log scale and are listed with 95% confidence interval for cancer types with a statistically significant association. H.R. > 1 indicates increased risk (decreased survival) and H.R. < 1 indicates decreased risk (increased survival). P-values are adjusted for age and tumor stage.

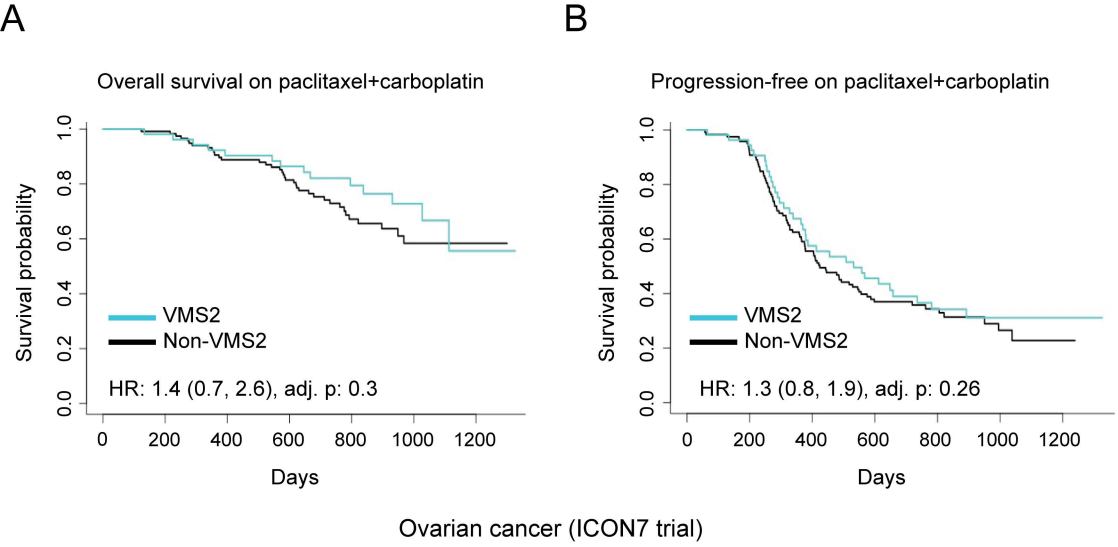


Ovarian cancer (ICON7 trial)

Supplemental Figure 10

**Supplemental Figure 10. VMS2 classification does not predict response to standard chemotherapy.**

Kaplan-Meier analysis comparing overall survival (**A**) and progression free survival (**B**) in ovarian cancer patients with VMS2 and non-VMS2 tumors on paclitaxel and carboplatin. HR = hazard ratio relating to the therapy. All p-values are the result of multivariate Cox regression analysis with patient age and tumor stage as covariates.

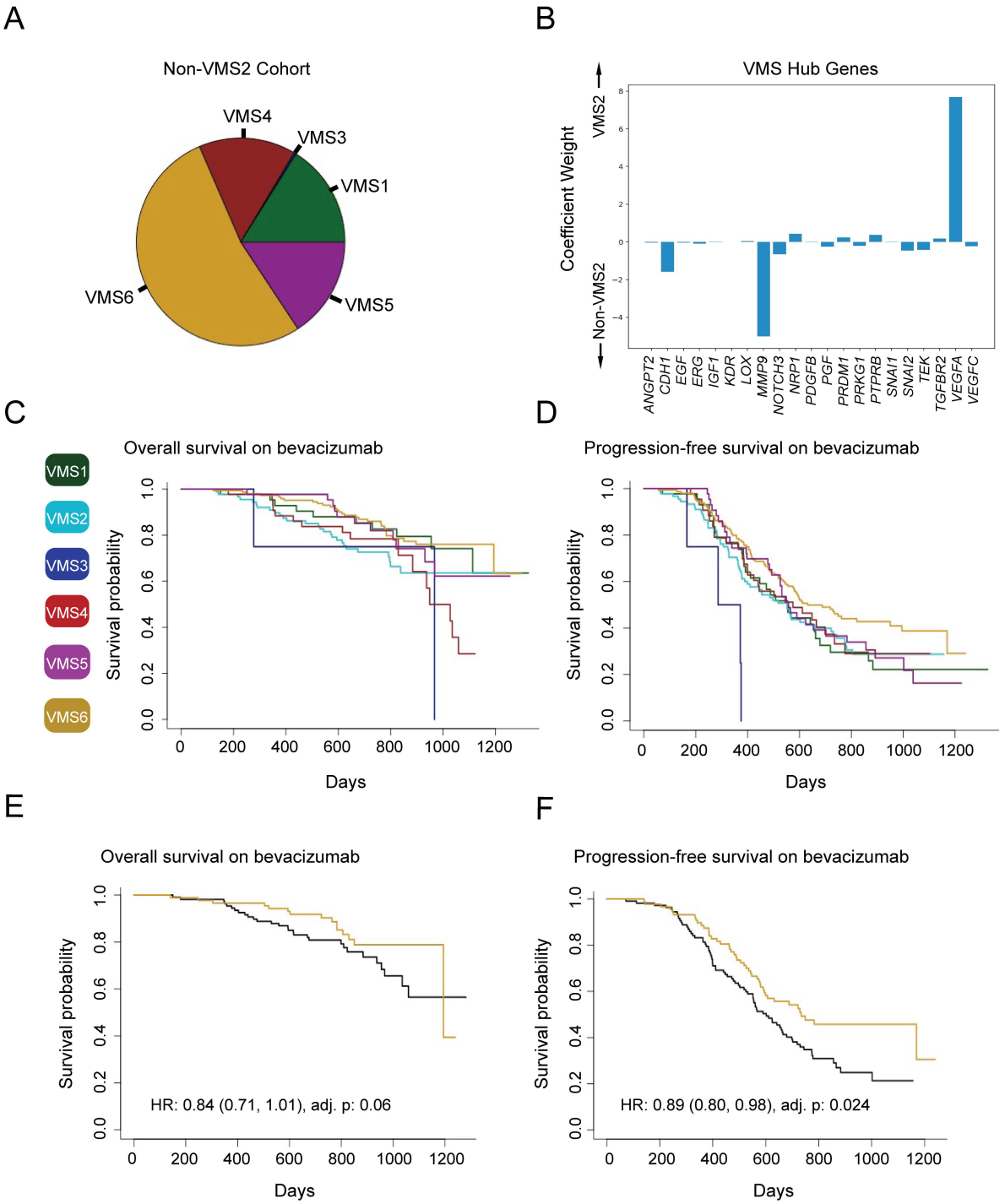


Supplemental Figure 11

**Supplemental Figure 11. Patients with VMS6 tumors respond favorably to bevacizumab**

(**A**) Pie chart showing the specific VMS composition of non-VMS2 cohort. (**B**) Bar plot shows the contribution of each of the 24 hub genes to the VMS2 classifier. Genes with positive values influence the classifier towards a VMS2 classification, and genes with negative values influence the classifier towards a non-VMS2 classification. Kaplan Meier plots show the overall (**C**) and progression-free (**D**) survival curves for patients classified as VMS1-6. Kaplan-Meier analysis comparing overall survival (**E**) and progression free survival (**F**) in ovarian cancer patients with VMS6 and non-VMS6 tumors on bevacizumab. HR = hazard ratio relating to the therapy. All p-values are the result of multivariate Cox regression analysis with patient age and tumor stage as covariates.